Journal of Siberian Federal University. Chemistry 1 (2008) 24-34
~ ~ ~

УДК 543.085 8

Evidence for CO Disproportionation over Ceria during Oxygen Storage Capacity Measurements: an in Situ Raman Spectroscopic Investigation

Meghan Swanson, Vladimir V. Pushkarev, Vladimir I. Kovalchuk* and Julie L. d'Itri
Department of Chemical and Petroleum Engineering, University of Pittsburgh, Pittsburgh, PA 15261 [1]

Received 15.01.2008, received in revised form 15.03.2008, accepted 10.04.2008

The interaction of CO with ceria under conditions typical for oxygen storage capacity (OSC) measurements of three way catalysts (TWC) has been investigated by in situ Raman spectroscopy. It has been shown that CO disproportionates over ceria at 623 K to deposit disordered carbon nano-crystallites, with calculated average crystal size of less than 20 Å. Exposure of the carbonized ceria to gaseous O_2 at room temperature resulted in the disappearance of the bands attributed to the carbon in Raman spectra, accompanied by the emerging of bands of surface formates, carbonates, and adsorbed peroxide species. Even though the kinetics of the ceria-catalyzed CO disproportionation reaction has yet to be measured, the present investigation suggests that the generally accepted procedure for OSC measurements of TWCs results in an OSC overestimation and, hence, needs to be reconsidered.

Keywords: CO disproportionation, carbonaceous deposits, ceria, oxygen storage capacity, situ Raman spectroscopy.

Introduction

Ceria is a critical component in automotive three way catalysts (TWC). It inhibits thermal sintering of noble metals and promotes the water gas shift reaction, which oxidizes CO with water during fuel-rich excursions [1]. Cerium in its oxide is also able to oscillate between the Ce^{3+} and Ce^{4+} oxidation states. Thus, the oxygen "stored" under oxidizing conditions is utilized to convert CO and hydrocarbons to CO_2 under reducing conditions. Generally, TWCs without cerium operate efficiently over a narrow stoichiometric range of air to fuel, so addition of ceria allows wider oscillations in the air to fuel ratios over which CO and hydrocarbons are oxidized and NO_x is reduced [1]. This increases the efficiency of the exhaust pollutant destruction over a range of driving conditions.

An important factor in TWC performance, therefore, is the catalyst's oxygen storage capacity (OSC). Ongoing development of improved TWCs relies on the accurate determination of OSC. An established technique for measuring the amount of stored oxygen involves pulse injection experiments [2,3] in which the catalyst is exposed to oxygen pulses, followed by one or more CO pulses. The total amount of CO_2 produced after alternating single pulses of O_2 and CO is termed

* Corresponding author E-mail address: vkovalchuk@mckasd.net

the OSC [4]. When a fully oxidized sample is exposed to consecutive pulses of CO until CO_2 production ceases, the total amount of CO_2 produced is called the OSC complete (OSCC) [4]. The OSC results vary with the reaction conditions such as the temperature, reactant partial pressures, and total pressure [2]. Typical OSC measurements are performed at 570-770 K with 1-10% O_2 and 1-5% CO in an inert gas [4,5]. In essence, the OSC is the amount of labile oxygen available for oxidation reactions under defined conditions.

Any reaction of CO with ceria that alters the concentration of CO_2 besides the reaction with labile oxygen decreases the accuracy of the OSC measurement. For example, if CO_2 adsorbs on the catalyst surface as carbonates, an underestimation of the OSC will be obtained. However, the effect of the carbonate formation during the OSC measurement can easily be taken into consideration because the carbonates decompose to form CO_2 upon a O_2 pulse following the CO pulse [6]. If CO_2 is produced without participation of labile oxygen species, the OSC can be overestimated. An example of such a reaction is CO disproportionation. This reaction results in the CO_2 formation and carbon deposition on the catalyst surface during the CO pulse and in the formation of an additional amount of CO_2 from the surface carbon oxidation, along with the formation of CO_2 from the carbonate decomposition, during the subsequent O_2 pulse.

The CO disproportionation reaction, also known as Boudouard's reaction, is thermodynamically feasible at temperatures below 1000 K, but kinetically insignificant in the absence of a catalyst [7]. With a transition metal-containing catalyst, the rate of CO disproportionation is appreciable [8,9]. Gredig *et. al.* [10] exposed Pd/ZrO_2 to 1730 ppm CO in Ar at 443 K for 18 h and observed XRD patterns consistent with carbon incorporation into the Pd lattice, which they attributed to CO disproportionation. As well with Pd supported on single crystal α-alumina, H_2 TPR showed methane offgassing following exposure to 3.8×10^{-5} Torr CO at 473 K [11]. It was surmised that CO disproportionation was responsible for the residual carbon on the Pd/ α-Al_2O_3 surface.

There is also indirect evidence that the reaction occurs over ceria-containing materials. During conventional OSC measurements, Holmgren et. al. [3] concluded that CO disproportionation explained the large amount of CO_2 produced over Pt/CeO_2, and smaller amounts produced on pure CeO_2. Li *et. al*. [12] exposed reduced metal free ceria to 30 Torr CO at room temperature and observed adsorbed carbonate species in infrared spectra. Since several bands had the same position and relative intensity as those formed after CO_2 exposure, CO disproportionation was inferred because CO_2 could not have been produced through CO oxidation by the pre-reduced ceria surface. However, to our best knowledge there is no direct evidence in the literature of surface carbon formation by CO disproportionation on ceria. Recently, a Raman spectroscopy investigation also provided results and interpretation consistent with the disproportionation of CO on CeO_2, although the discerned bands were not unambiguously attributed to carbonaceous deposits [13].

Thus, the objective of the present investigation was to probe the possibility of CO disproportionation over ceria under conditions of OSC measurements by means of *in situ* Raman spectroscopy. Raman spectroscopy is an appropriate method for the specified objective because graphite and other carbonaceous moieties are good Raman scatterers with very characteristic spectra [14].

Experimental

Cerium dioxide (> 99.9%) was supplied by Rhodia. Prior to use, CeO_2 was calcined in air at 823 K for 12 h in a standard muffle furnace. The BET surface area, average pore diameter, and

pore volume after calcination, measured by N_2 physisorption at 77 K with ASAP 2010 volumetric sorption analyzer (Micromeritics), were 127 m^2 g^{-1}, 4.8 nm, and 0.20 cm^3 g^{-1}, respectively. The average crystallite size determined from the (111) and (220) XRD lines broadening using the Scherrer equation was 9.7 nm.

The reagent grade He (Air Products, > 99.998%) was purified of water and oxygen traces by passing it through a deoxidant OxyTrap filter and through a 0.5-nm molecular sieve column (both Alltech). The CO (Praxair, >99.995%) was fitted with a Vista B γ-alumina trap, heated to 573 K, in order to remove metal carbonyl contaminants. The 10% O_2 in He (Praxair) was used without further purification.

The Raman spectra were acquired using a Renishaw System 2000 confocal Raman spectrometer equipped with a Leica DMLM microscope and a 514.5-nm Ar^+ ion laser as the excitation source. The laser power at the source was in the range of 5-25 mW, which caused minimal sample damage. An Olympus × 50 objective was used to focus the unpolarized laser beam onto a < 3 μm spot on the sample, and to collect the backscattered light. Ten scans were collected for each spectrum in the 100-4000 cm^{-1} range, at a resolution of 4 cm^{-1}. The *in-situ* Raman measurements were conducted at atmospheric pressure in a THMS 600 Raman cell from Linkam Scientific. Approximately 100 mg of catalyst was placed on a thin microscope slide, which was mounted into the cell.

The CO and He were mixed prior to the Raman cell. The desired flow rate of each gas (CO, He, and 10% O_2 in He) was maintained within ± 1 cm^3 min^{-1} using Brooks mass flow controllers (model 5850E). The total gas flow rate through the cell was 100 cm^3 min^{-1} for all treatments and experiments, and the heating/cooling rate was always 10 K min^{-1}.

The sample pretreatment consisted of heating the sample from room temperature to 673 K in 10% CO/He, and maintaining these conditions for 1 h. Subsequently, the flow was changed to 10% O_2/He at 673 K for 1 h. Finally, the sample was cooled to 623 K in 10% O_2/He flow, purged with pure He, and exposed to a 10% CO/He flow for the specified time. Prior to the exposure of the CO treated ceria sample to O_2, the pretreated sample was cooled to 298 K in a 10% CO/He flow and then exposed to a 10% O_2/He flow at the same temperature.

Results

After the oxidized ceria sample was exposed to CO for 1 h at 623 K, several new bands appeared in the Raman spectrum, while the bands characteristic of ceria decreased in intensity (Fig. 1). Characteristic ceria features include the band at 1166 cm^{-1}, which has been assigned to a mixing of the A_{1g}, E_g, and F_{2g} modes of ceria lattice vibrations [15], and the band at 3634 cm^{-1}, which has been attributed to the stretching mode of a ceria hydroxyl group vibration with bidendate coordination [16]. Both ceria bands decreased in intensity to approximately one quarter of the original value after 1 h exposure to CO at 623 K (Fig. 1). Concomitantly, new bands appeared at 2115 cm^{-1} and 1582 cm^{-1}, and a low-frequency shoulder formed on the 1166 cm^{-1} band at 1068 cm^{-1}. The band at 2115 cm^{-1} has been assigned to the symmetry-forbidden $^2F_{5/2} \rightarrow {}^2F_{7/2}$ electronic transition of Ce^{3+} [17].

The temporal development of Raman spectral features on a pretreated ceria sample during 24 h of CO exposure at 623 K is shown in Fig. 2. After 20 minutes, low-intensity bands appeared at 2115 cm^{-1}, and at 1068 cm^{-1} as a low-frequency shoulder of the 1166 cm^{-1} band. After 205 minutes, new bands appeared at 1582, 1434, and 1331 cm^{-1}. After 1040 minutes, an additional broad feature centered at 2840 cm^{-1}

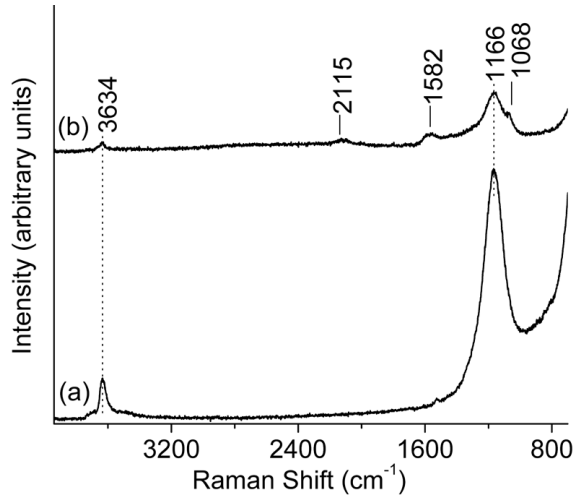

Fig. 1. *In situ* Raman spectra of CeO_2 (a) after treatment in 10% O_2/He at 673 K for 1 h and (b) after exposure to 10% CO/He at 623 K for 1 h. All spectra were recorded at 623 K

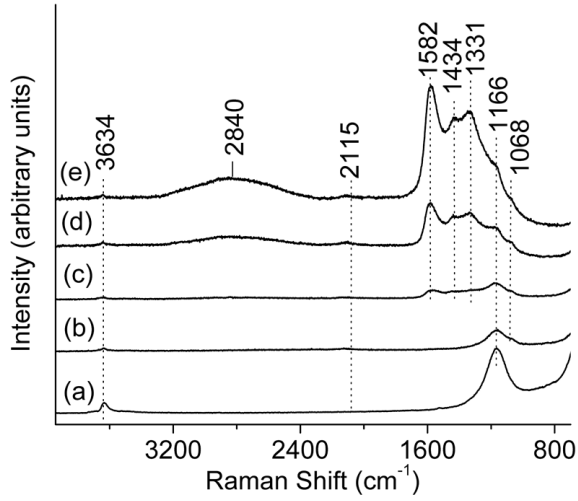

Fig. 2. I*n situ* Raman spectra of CeO_2 exposed to a flow of 10% CO/He at 623 K for: (a) 0 min, (b) 20 min, (c) 205 min, (d) 1040 min, and (e) 1300 min. All spectra were recorded at 623 K

was observed. The characteristic ceria bands, at 3634 and 1166 cm^{-1}, as well as the new bands at 2115 and 1068 cm^{-1} formed after the 20 minute CO exposure, all retained consistent intensities after formation. Conversely, the intensities of the new bands at 1582, 1434, and 1331 cm^{-1}, which all became detectable after 205 minutes of CO exposure, continued to increase with prolonged CO exposure, up to 1300 minutes.

A separate ceria sample was treated in CO at 623 K for 12 h and cooled to room temperature. A band observed at 1174 cm^{-1} (Fig. 3, spectrum a) is attributed to the same ceria lattice vibrations, a combination of the A_{1g}, E_g, and F_{2g} modes, that were observed at 1166 cm^{-1} in Fig. 1 and 2. The band has shifted because of the change in temperature, from 623 to 298 K, at which the spectrum was collected. As the ceria was cooled, lattice bonds shrank because of thermal contraction, with an accompanying increase in the lattice bond energy. This caused the vibrational bands to shift to a higher wavenumber [18,19]. Similar to the bands

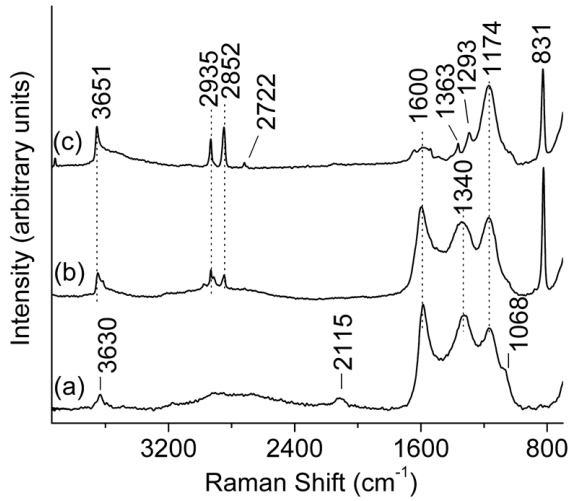

Fig. 3. *In situ* Raman spectra of CeO_2 (a) treated in a flow of 10% CO/He at 623 K for 12 h followed by exposure to a flow of 10% O_2/ He at 298 K for (b) 30 min, and (c) 12 h. All spectra were recorded at 298 K

previously seen in Fig. 1 and 2, after 12 h CO exposure the band of the $^2F_{5/2} \rightarrow {}^2F_{7/2}$ electronic transition and the hydroxyl bands were observed at 2115 and 3630 cm^{-1}, respectively. Additionally, bands were observed at 1600, 1340, and 1068 cm^{-1} that could not be assigned to ceria.

When the same ceria sample was exposed to oxygen at room temperature, within 30 minutes a band appeared at 831 cm^{-1}, in addition to bands at 2852 and 2935 cm^{-1} (Fig. 3(b)). The band at 831 cm^{-1} has been assigned to surface peroxide [20], and the 2852 and 2935 cm^{-1} bands are consistent with formate species previously observed in infrared spectra of ceria partially reduced in hydrogen at 673 K for 1 h [21]. The 2852 cm^{-1} formate band was assigned to a combination of the C-H bend and O-C-O asymmetric stretch, while the 2935 cm^{-1} band was assigned to the C-H stretch [21,22].

After 12 h, the bands at 1340 and 1600 cm^{-1} had dramatically decreased in intensity (Fig. 3(c)). At this time new peaks were also visible at 2722, 1363, and 1293 cm^{-1}, in addition to low intensity, broad peaks in the vicinity of 1600 cm^{-1}. As well, the intensity of the formate peaks at 2935 and 2852 cm^{-1} and the ceria hydroxyl peak at 3651 cm^{-1} increased after 12 h oxygen exposure. The 2722 cm^{-1} band was assigned previously in infrared spectra of ceria partially reduced in hydrogen at 673 K for 1 h to a formyl species [21]. It appeared after long exposure times because formyl is a possible intermediate to formate formation from ceria hydroxyls. After formate approaches saturation, the reverse reaction stabilizes the formyl formation [21-24].

Formate also exhibits strong infrared bands at 1599, 1553, and 1542 cm^{-1}, all assigned to the O-C-O asymmetric stretch [22]. Their appearance can explain the broad, low intensity peaks formed around 1600 cm^{-1} after 12 h O_2 exposure (Fig. 3(c)) [21-23]. Additionally, the band that appeared at 1363 cm^{-1} after 12 h O_2 exposure (Fig. 3(c)) was assigned to a formate asymmetric O-C-O stretching vibration [21-23].

Discussion

The Raman spectroscopy results presented in this work are consistent with the formation of surface carbon on ceria. This suggests that CO disproportionates on ceria under reaction conditions relevant to oxygen storage capacity measurements for automotive catalysis. The

thermodynamics of CO disproportionation are favorable below 1000 K, but the reaction is kinetically insignificant without a catalyst [7]. Thus, the most important results to evaluate in the context of this hypothesis are the formation of bands during exposure to CO (Fig. 1-3) and the decrease in intensity of those bands when exposed to O_2 at room temperature (Fig. 3).

The frequency of the band at 1582 cm^{-1} (Fig. 1-2) formed during CO exposure at 623 K is the same as the fundamental carbon stretching mode in graphite and other sp^2 hybridized carbon structures [25-30], the Raman-active E_{2g} mode [31]. This mode is referred to as the G (graphite) band, and unflawed single graphite crystals larger than about 200 Å exhibit only the G band [25-30]. The band shifts to 1600 cm^{-1} at room temperature (Fig. 3). As the temperature decreases the lattice bond energy increases, which results in a higher characteristic Raman vibration, similar to the 1166 cm^{-1} ceria lattice mode.

The frequency of the band at 1331-1340 cm^{-1} (Fig. 2-3) is comparable to literature values reported for disordered carbon, namely, the D band. This band arises from the breathing mode of A_{1g} symmetry; it is forbidden in perfect large crystals, but is allowed by the disorder induced in small graphite moieties [27-30,32,33]. Polycrystalline graphite and other sp^2 carbon structures exhibit the D band at around 1332 cm^{-1}, in addition to the G band [27-30]. The shift of the D band with temperature (Fig. 2-3) may be caused by a thermal relaxation of the lattice vibrations, similar to the G band and the ceria lattice mode. The broad band at 2800 cm^{-1} (Fig. 2-3) is an overtone of the D band. More ordered carbon forms, such as glassy carbon, have a sharp overtone at 2710 cm^{-1} [27]. However, investigations with activated carbon and carbon black showed that the overtone broadens as disorder increases [25,27,30,31,34].

Additionally, the behavior of the 1434 cm^{-1} band (Fig. 2) indicates that it may also be attributed to carbon. The band intensity increased with exposure to CO at the same rate as the G and D bands in Fig. 2. It should be noted that the distinct peak at 1434 cm^{-1} was not observed after 12 h exposure of another ceria sample to CO at 623 K (Fig. 3). However, the features of the spectra "a" and "b" in Fig. 3 indicate that the 1434 cm^{-1} band is present but of a smaller relative intensity than in Fig. 2, and is obscured by a broad band at 1340 cm^{-1}. This sample to sample variation may indicate that the band at 1434 cm^{-1} is caused by a geometric effect, such as interaction with the ceria substrate. Further studies are needed to assign confidently the feature at 1434 cm^{-1}.

There are several reasons to exclude carbonates in the assignment of the 1582-1600 cm^{-1} and 1331-1340 cm^{-1} bands, even though it is well established that carbonates will form on ceria at conditions similar to those used in the present work [3,35]. The species contributing to the 1582-1600 cm^{-1} and 1331-1340 cm^{-1} vibrational bands readily react with O_2 at room temperature (Fig. 3), which is uncharacteristic of carbonate species. The bands at 1600 and 1340 cm^{-1} decreased over 90% after exposure to oxygen for 12 h, as shown in Fig. 3(c), but carbonates of ceria should be stable in oxygen at room temperature. Indeed, carbonate species have been observed on ceria even after evacuation to the pressure of 10^{-4} Torr at 773 K, and outgassing temperatures of 1000 K are commonly used to decompose them on the ceria surface [36,37].

However, one Raman band in this investigation is most reasonably assigned to the formation of a carbonate from the reaction of CO with the ceria surface; namely, the band at 1068 cm^{-1} (Fig. 1-3). The band increases in intensity during the first 20 minutes of exposure to CO, and unlike the bands at 1582-1600 cm^{-1} and 1331-1340 cm^{-1}, the 1068 cm^{-1} band does not change in intensity thereafter. In a separate Raman experiment in this laboratory, stoichiometric

cerium(III) carbonate exhibited a strong doublet at 1086 and 1077 cm^{-1}. Bulk carbonate has several IR bands between 1600 and 800 cm^{-1}, and studies have attributed a peak in the 1073-1062 cm^{-1} region to bulk cerium carbonate [16,17,36-38].

It is worthwhile to consider the chemistry that occurs when the carbon, formed on ceria after 12 h CO treatment, is exposed to oxygen at room temperature. Formate species form, probably via the reaction of carbon with adsorbed dioxygen and ceria hydroxyls. Formate species were observed elsewhere [21] by means of IR spectroscopy on partially reduced in H_2 ceria at room temperature upon exposure to CO. This indicates that the first step in formate formation is surface reduction, which in the present study could be accomplished with CO. A possible reaction scheme for the formation of formates is shown below:

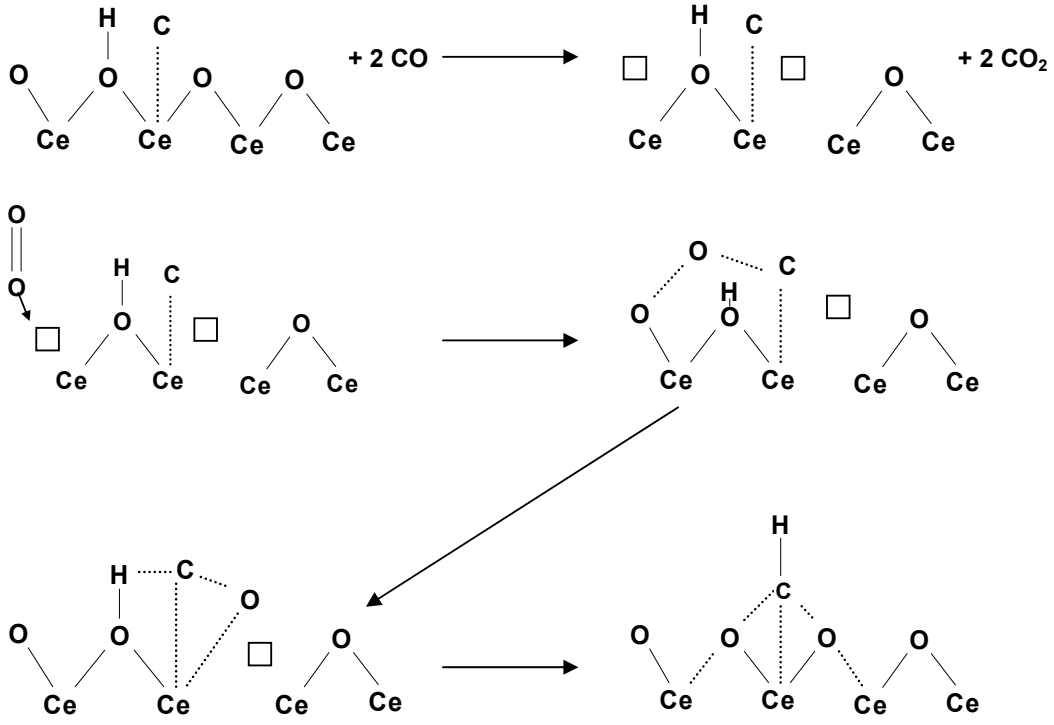

As well, surface ceria carbonates form several peaks in the 1562-1286 cm^{-1} region [3,12,17,21,37-39]. For instance, the band that appeared at 1293 cm^{-1} after 12 h O_2 exposure (Fig. 3) is consistent with an IR band at 1286 cm^{-1} assigned to bidendate carbonate [36].

Clearly, the carbon formed from CO disproportionation is highly reactive as it reacts with oxygen at room temperature. One indication of reactivity may be the degree of disorder of the carbon deposits. The degree of disorder should correlate with average graphite crystal size. A decrease in crystal size results in an increase in the number of edges and corners in the graphite microcrystals, which may correspond to the number of active, coordinatively unsaturated sites.

The degree of disorder may be approximated by the position and relative intensities of the G and D bands. The band locations are similar for variety of sp^2-hybridized carbon materials such as graphite [29], glassy carbon [28], carbon nanotubes [34], carbon black [14], and activated carbon [40]. As the carbon becomes more disordered, the D band

appears, the G band broadens and shifts toward higher wavenumbers [30,41], and the width of the second order band at 2800 cm^{-1} increases [30]. For graphite, the relationship between the D and G band intensities, measured with 514.4 nm excitation, and particle size is expressed as $I_G/I_D = 44$ Å$/L_a$, where L_a is the size of the graphite plane [29,30]. It is possible to calculate L_a in the current study, but one must keep in mind that the empirical relationship is not valid for amorphous carbon [29,42,43]. Additionally, the minimum L_a that has been experimentally verified is approximately 20 Å [44]. According to Nistor *et. al.* [45], the spectrum of fully developed carbon in Fig. 2(e) was deconvoluted and fit with two Lorentzian peaks at the D and G bands, as well as a Gaussian line for the broad band at 1500 cm^{-1} for amorphous sp^2 carbon (not shown). The microcrystalline size was calculated as 17 Å, which is below the experimentally verified range of the equation. This value does, however, indicate that the carbon exhibits a high degree of disorder.

Conclusions

It has been shown that CO disproportionates over noble metal free ceria under conditions of OSC measurements. Carbon formed from CO disproportionation exhibits a high degree of disorder and oxidizes by oxygen at room temperature. These results suggest that CO disproportionation should be taken into account when performing OSC measurements on ceria-containing catalysts because additional amounts of CO_2 are produced without involvement of the labile lattice ceria oxygen. However, the kinetics of the CO disproportionation reaction must still be investigated in order to estimate quantitatively the impact of the disproportionation reaction on the results of OSC measurements.

Acknowledgements

Support from National Science Foundation (CTS 0086638) is gratefully acknowledged.

References

[1] Kaspar J., Fornasiero P., Graziani, M. Use of CeO_2-based oxides in the three-way catalysis. Catal. Today. 1999. Vol. 50. N 2. P. 285-298.

[2] Bedrane S., Descorme C., Duprez D. Investigation of the oxygen storage process on ceria- and ceria-zirconia-supported catalysts. Catal. Today. 2002. Vol. 75. N 1-4. P. 401-405.

[3] Holmgren A., Andersson B., Duprez D. Interactions of CO with Pt/ceria catalysts. Appl. Catal. B. 1999. Vol. 22. N 3. P. 215-230.

[4] Yao H., Yu Yao, Y. Ceria in automotive exhaust catalysts. 1. Oxygen storage. J. Catal. 1984. Vol. 86. N 2. P. 254-265.

[5] Holmgren A., Andersson B. Oxygen storage dynamics in $Pt/CeO_2/Al_2O_3$ catalysts. J. Catal. 1998. Vol. 178. N 1. P. 14-25.

[6] Sharma S., Hilaire S., Vohs J.M., Gorte R.J., Jen H.W. Evidence for Oxidation of Ceria by CO_2. J. Catal. 2000. Vol. 190. N 1 P. 199-204.

[7] Cheng, H., Reiser D.B., Dean S., Jr. On the mechanism and energetics of Boudouard reaction at FeO(100) surface $2CO \rightarrow C+CO_2$. Catal. Today. 1999. Vol. 50. N 3-4. P. 579-588.

[8] Frusteri F., Spadaro L., Arena F., Chuvilin A. TEM evidence for factors affecting the genesis of carbon species on bare and K-promoted Ni/MgO catalysts during the dry reforming of methane. Carbon. 2002. Vol. 40. N 7. P. 1063-1070.

[9] Snoeck J.W., Froment G.F., Fowles M. Steam/CO_2 Reforming of Methane. Carbon Filament Formation by the Boudouard Reaction and Gasification by CO_2, by H_2, and by Steam: Kinetic Study. Ind. Eng. Chem. Res. 2002. Vol. 41. N 17. P. 4252-4265.

[10] Gredig S., Tagliaferri M., Maciejewski M., Baiker A. Oxidation and disproportionation of carbon monoxide over Pd/ZrO_2 catalysts prepared from glassy Pd-Zr alloy and by co-precipitation. Stud. Surf. Sci. Catal. 1995. Vol. 96. P. 285-294.

[11] Ichikawa S., Poppa H., Boudart M. The effect of particle size on the reactivity of supported palladium. in: Catalytic Materials: Relationship between Structure and Reactivity (T.E. Whyte, Jr. et al., Eds.), ACS Symp. Ser. Vol. 248. 1984. P. 439-451.

[12] Li C., Sakata Y., Arai T., Domen K., Maruya K., Onishi T. Carbon monoxide disproportionation at mild temperatures over partially reduced cerium oxide. J. Chem. Soc., Chem. Commun. 1991. N 6. P. 410-411.

[13] Swanson M., Pushkarev V.V., Kovalchuk V.I., d'Itri J.L. The dynamic surface chemistry during the interaction of CO with ceria captured by Raman spectroscopy. Catal. Lett. 2007. Vol. 116. N 1-2. P. 41-45.

[14] Jawhari T., Roid A., Casado J. Raman spectroscopic characterization of some commercially available carbon black materials. Carbon. 1995. Vol. 33. N 11, P. 1561-1565.

[15] Weber. W., Hass K., McBride J. Raman study of CeO_2: second-order scattering, lattice dynamics, and particle-size effects. Phys. Rev. B. 1993. Vol. 48. N 1. P. 178-185.

[16] Laachir A., Perrichon V., Badri A., Lamotte J., Catherine E., Lavalley J.C., El Fallah J., Hilaire L., Le Normand F. Reduction of cerium dioxide by hydrogen. Magnetic susceptibility and Fourier-transform infrared, ultraviolet and x-ray photoelectron spectroscopy measurements. J. Chem. Soc., Faraday Trans. 1991. V. 87. N 10. P. 1601-1609.

[17] Binet C., Badri A., Lavalley J.C. A Spectroscopic Characterization of the Reduction of Ceria from Electronic Transitions of Intrinsic Point Defects. J. Phys. Chem. 1994. Vol. 98. N 25. P. 6392-6398.

[18] Ichikawa S., Suda J., Sato T., Suzuki Y. Lattice dynamics and temperature dependence of the first-order Raman spectra for α-SiO_2 crystals. J. Raman Spectrosc. 2003. Vol. 34. N 2. P. 135-141.

[19] Bertheville B., Bill H. The temperature dependence of the Raman T_{2g} lattice mode in K_2S crystals. Solid State Ionics. 2001. Vol. 139. N 1-2. P. 159-162.

[20] Pushkarev V.V., Kovalchuk V.I., d'Itri J.L. Probing Defect Sites on the CeO_2 Surface with Dioxygen. J. Phys. Chem. B. 2004. Vol. 108. N 17. P. 5341-5348.

[21] Li C., Sakata Y., Arai T., Domen K., Maruya K., Onishi, T. Adsorption of carbon monoxide and carbon dioxide on cerium oxide studied by Fourier-transform infrared spectroscopy. 2. Formation of formate species on partially reduced cerium dioxide at room temperature. J. Chem. Soc., Faraday Trans. 1. 1989. Vol. 85. N 6. P. 1451-1461.

[22] Li C., Domen K., Maruya K., Onishi T. Spectroscopic identification of adsorbed species derived from adsorption and decomposition of formic acid, methanol, and formaldehyde on cerium oxide. J. Catal. 1990. Vol. 125. N 2. P. 445-455.

[23] Lavalley J.C., Saussey J., Raïs T. Infrared study of the interaction between CO and H_2 on ZnO: Mechanism and sites of formation of formyl species. J. Mol. Catal. 1982. Vol. 17. N 2-3. P. 289-298.

[24] Saussey J., Lavalley J.C., Lamotte J., Rais T. I.R. Spectroscopic evidence of formyl species formed by CO and H_2: Co-adsorption on ZnO and Cu-ZnO. J. Chem. Soc., Chem. Commun. 1982. N 5. P. 278-279.

[25] Wang Y., Alsmeyer D.C., McCreery R.L. Raman spectroscopy of carbon materials: structural basis of observed spectra. Chem. Mater. 1990. Vol. 2. N 2. P. 557-53.

[26] Dillon R.O., Woollam J.A. Use of Raman scattering to investigate disorder and crystallite formation in as-deposited and annealed carbon films. Phys. Rev. B. 1984. Vol. 29. N 6. P. 3482-3489.

[27] Nemanich R.J., Solin S.A. First- and second-order Raman scattering from finite-size crystals of graphite. Phys. Rev. B. 1979. Vol. 20. N 2. P. 392-401.

[28] Nathan M.I., Smith J.E., Tu K.N. Raman spectrum of glassy carbon. J. Appl. Phys. 1974. Vol. 45. N 5. P. 2370-2371.

[29] Tuinstra F., Koenig J.L. Raman spectrum of graphite. J. Chem. Phys. 1970. Vol. 53. N 3. P. 1126-1130.

[30] Knight D.S., White W.B. Characterization of diamond films by Raman spectroscopy. J. Mater. Res. 1989. Vol. 4. N 2. P. 385-393.

[31] Al-Jishi R., Dresselhaus G. Lattice-dynamical model for graphite. Phys. Rev. B. 1982. Vol. 26. N 8. P. 4514-4522.

[32] Matthews M.J., Pimenta M.A., Dresselhaus G., Dresselhaus M.S., Endo M. Origin of the dispersive effects of the Raman D band in carbon materials. Phys. Rev. B. 1999. Vol. 59. N 10. P. R6585-R6588.

[33] Póscik I., Hundhausen M., Koós M., Ley L. Origin of the D peak in the Raman spectrum of microcrystalline graphite. J. Non-Cryst. Solids. 1998. Vol. 227-230. Part 2. P. 1083-1086.

[34] Kastner J., Pichler T., Kuzmany H., Curran S., Blau W., Weldon D. N., Delamesiere M., Draper S., Zandbergen H. Resonance Raman and infrared spectroscopy of carbon nanotubes. Chem. Phys. Lett. 1994. Vol. 221. N 1-2. P. 53-58.

[35] Zhao S., Luo T. Gorte R. J. Deactivation of the water-gas-shift activity of Pd/ceria by Mo. J. Catal. 2004. Vol. 221. N 2. P. 413-420.

[36] Li C., Sakata Y., Arai T., Domen K., Maruya K., Onishi T. Carbon monoxide and carbon dioxide adsorption on cerium oxide studied by Fourier-transform infrared spectroscopy. 1. Formation of carbonate species on dehydroxylated cerium dioxide at room temperature. J. Chem. Soc., Faraday Trans. 1. 1989. Vol. 85. N 4. P. 929-943.

[37] F. Bozon-Verduraz F., Bensalem A. IR studies of cerium dioxide: influence of impurities and defects. J. Chem. Soc., Faraday Trans. 1994. Vol. 90. N 4. P. 653-657.

[38] Binet C., Badri A., Boutonnet-Kizling M., Lavalley J. C. FTIR study of carbon monoxide adsorption on ceria: CO_2^{2-} carbonite dianion adsorbed species. J. Chem. Soc., Faraday Trans. 1994. Vol. 90. N 7. P. 1023-1028.

[39] Bensalem A., Muller J.C., Tessier D., Bozon-Verduraz F. Spectroscopic study of CO adsorption on palladium-ceria catalysts. J. Chem. Soc., Faraday Trans. 1996. Vol. 92. N 17. P. 3233-3237.

[40] Sze S.K., Siddique N., Sloan J.J., Escribano R. Raman spectroscopic characterization of carbonaceous aerosols. Atmospheric Environment. 2000. Vol. 35. N 3. P. 561-568.

[41] Yoshikawa M., Nagai N., Matsuki M., Fukuda H., Katagiri G., Ishida H., Ishitani A. Raman scattering from sp^2 carbon clusters. Phys. Rev. B. 1992. Vol. 46. N 11. P. 7169-7174.

[42] Schwan J., Ulrich S., Batori V., Ehrhardt H., Silva S. R. P. Raman spectroscopy on amorphous carbon films. J. Appl. Phys. 1996. Vol. 80. N 1. P. 440-447.

[43] Castiglioni C., Mapelli C., Negri F., Zerbi G. Origin of the D line in the Raman spectrum of graphite: A study based on Raman frequencies and intensities of polycyclic aromatic hydrocarbon molecules. J. Chem. Phys. 2001. Vol. 114. N 2. P. 963-974.

[44] Ferrari A. C., Robertson J. Interpretation of Raman spectra of disordered and amorphous carbon. Phys. Rev. B. 2000. Vol. 61. N 20. P. 14095-14107.

[45] Nistor L.C., Van Landuyt J., Ralchenko V.G., Kononenko E.D., Obraztsova V.E., Strelnisky V. E. Direct observaton of Laser-induced crystallizaton of a-C:H films. Appl. Phys. A. 1994. Vol. 58. N 2. P. 137-144.